AFRL-AFOSR-UK-TR-2014-0032

Low-dose, chronic exposure to silver nanoparticles causes mild mitochondrial alterations in the liver of Sprague-Dawley rat

CARLOS PALMEIRA

CENTRO DE NEUROCIENCIAS E BIOLOGIA CELULAR (CNC)
DEPARTAMENTO DE ZOOLOGIA
COIMBRA 3000 - 329 PORTUGAL

EOARD Grant 13-3036

Report Date: May 2014

Final Report from 28 February 2013 to 27 February 2014

Air Force Research Laboratory
Air Force Office of Scientific Research
European Office of Aerospace Research and Development
Unit 4515, APO AE 09421-4515

REPORT DOCUMENTATION PAGE

Form Approved OMB No. 0704-0188

1. REPORT DATE *(DD-MM-YYYY)*	2. REPORT TYPE	3. DATES COVERED *(From – To)*
10 May 2014	Final Report	28 February 2013 – 27 February 2014

4. TITLE AND SUBTITLE

Low-dose, chronic exposure to silver nanoparticles causes mild mitochondrial alterations in the liver of Sprague-Dawley rat

5a. CONTRACT NUMBER

FA8655-13-1-3036

5b. GRANT NUMBER

Grant 13-3036

5c. PROGRAM ELEMENT NUMBER

61102F

6. AUTHOR(S)

CARLOS PALMEIRA

5d. PROJECT NUMBER

5d. TASK NUMBER

5e. WORK UNIT NUMBER

7. PERFORMING ORGANIZATION NAME(S) AND ADDRESS(ES)

CENTRO DE NEUROCIENCIAS E BIOLOGIA CELULAR (CNC)
DEPARTAMENTO DE ZOOLOGIA
COIMBRA 3000 - 329 PORTUGAL

8. PERFORMING ORGANIZATION REPORT NUMBER

N/A

9. SPONSORING/MONITORING AGENCY NAME(S) AND ADDRESS(ES)

EOARD
Unit 4515
APO AE 09421-4515

10. SPONSOR/MONITOR'S ACRONYM(S)

AFRL/AFOSR/IOE (EOARD)

11. SPONSOR/MONITOR'S REPORT NUMBER(S)

AFRL-AFOSR-UK-TR-2014-0032

12. DISTRIBUTION/AVAILABILITY STATEMENT

Distribution A: Approved for public release; distribution is unlimited.

13. SUPPLEMENTARY NOTES

14. ABSTRACT

Nanoparticles (NPs) are, by definition, materials that range in size from 1 to 100 nanometers, in at least one axis, which allows for a broad selection of shapes and sizes, from spheres to rods, tubes and more intricate shapes. The use of NPs has been steadily increasing worldwide due to their fascinating and particular physicochemical properties that wildly differ from the ones presented by the same materials, in a larger scale. Ranging from particular optic alterations to thermal and electric conductance and biological-affecting altered characteristics, these properties have been extensively studied and utilized in common situations in everyday life, from personal hygiene items, medical applications and industry processes. These derive from their particular size, shape, crystallinity, surface charge and possible coating, elemental composition and solubility. However, there is growing concern that the accumulation of NPs in an larger organism and on the environment could lead to pernicious effects, too soon to be fully detected and understood, but too late to prevent them. These effects might be consequence of the same properties that make them so attractive in the first place. As such, the importance of studying what effects might arise from this current unchecked use of NP cannot be stressed enough. From all types and shapes of NPs, silver NPs (AgNPs) are by far the most ubiquitous type of nanomaterial. Probably the best-known and more ancient use of silver (other than jewelry) derives from its antimicrobial properties, making AgNPs a most excellent mean of disinfection and sterilization. The results of the study described in this report show that even a low-dose, chronic exposure to AgNPs can cause severe impediments to normal mitochondrial function, at least at a hepatic level. Despite no alterations were found in heart and kidney levels, and despite the fact that the alterations found in liver mitochondria did not appear to compromise ATP generation, it is not possible (and, in fact, it is probably unadvisable) to rule out any harmful effects of AgNPs, even in a low dose, to the organism.

15. SUBJECT TERMS

EOARD, Nano particles, Photo-Acoustic Sensors

16. SECURITY CLASSIFICATION OF:			17. LIMITATION OF ABSTRACT	18, NUMBER OF PAGES	19a. NAME OF RESPONSIBLE PERSON
a. REPORT	b. ABSTRACT	c. THIS PAGE			James H Lawton, PhD
UNCLAS	UNCLAS	UNCLAS	SAR	23	19b. TELEPHONE NUMBER *(Include area code)* (703)696-5999

Low-dose, chronic exposure to silver nanoparticles causes mild mitochondrial alterations in the liver of Sprague-Dawley rats

1. Introduction:

Nanoparticles (NPs) are, by definition, materials that range in size from 1 to 100 nanometers, in at least one axis, which allows for a broad selection of shapes and sizes, from spheres to rods, tubes and more intricate shapes. The use of NPs has been steadily increasing worldwide due to their fascinating and particular physicochemical properties that wildly differ from the ones presented by the same materials, in a larger scale. Ranging from particular optic alterations to thermal and electric conductance and biological-affecting altered characteristics ([1]), these properties have been extensively studied and utilized in common situations in everyday life, from personal hygiene items, medical applications and industry processes. These derive from their particular size, shape, crystallinity, surface charge and possible coating, elemental composition and solubility ([2]). However, there is growing concern that the accumulation of NPs in an larger organism and on the environment could lead to pernicious effects, too soon to be fully detected and understood, but too late to prevent them ([3]). These effects might be consequence of the same properties that make them so attractive in the first place ([2]; [4]). As such, the importance of studying what effects might arise from this current unchecked use of NP cannot be stressed enough.

From all types and shapes of NPs, silver NPs (AgNPs) are by far the most ubiquitous type of nanomaterial ([5]). Probably the best-known and more ancient use of silver (other than jewelry) derives from its antimicrobial properties, making AgNPs a most excellent mean of disinfection and sterilization ([2]; [6]; [7]). As such, they have been, for the past few years, been widely used not only in medical devices, as wound dressings, catheters, contraceptives, bone prosthetics, surgical instruments, contrast agents, drug

delivery vehicles and biosensors ([7]; [8]), but also in common everyday products, as cosmetics, creams and lotions, toothpaste, soap, sunscreen, clothing and electronics ([7]; [4]).

Due to this ubiquity and concerns for public and environmental health issues, several studies have been conducted on the potential for injury by NPs exposure (for reviews on the matter, check [9]; [10]; [11]). These studies have identified some organs and structures as targets for NPs-induced toxicity, such as our previous work, focused on AgNPs acute liver mitochondrial effects ([4]). Other studies proved toxic effects on a panoply of organs, from brain, heart, skin, lungs, bone marrow, to name a few ([12];[13]). However, most of the studies published so far focused on either acute effects of exposure to AgNPs or on high levels of exposure. So far, to the best of our knowledge, no study has approached AgNPs toxicity in a chronic, low-dose treatment, with a focus on mitochondrial function.

Mitochondria are the eukaryotic cells' powerhouses, for they generate roughly 90% of the energy the cells utilizes, in the form of ATP ([14]). But the generation of ATP is one of the dozens of key roles mitochondria play in maintaining cell viability. As such, it comes as no surprise that the disruption of mitochondrial homeostasis is a key event in a wide variety of diseases and toxicological effects, and even normal events such as ageing ([15]; [16]). In terms of NPs toxicity, the link between NPs and mitochondria has already been tested and demonstrated, with a wide range of NPs source materials, such as gold ([17]), copper ([18]) and silver ([4]; [19]), to name a few. Most of these studies have concluded that the main mechanism by which NPs exert their nefarious effects is by ramping up the generation of reactive oxygen species (ROS), particularly at the mitochondrial level. However, this is not a consensual event, for some works (including our previous work on the matter, [4]) have failed to perceive a increase in mitochondrial ROS generation. And, as mentioned before, most of these studies were conducted *in vitro* or in an acute exposure setting, rendering to speculation if the exposure to a permanent low-dose of NPs can be harmful to fully developed organism. Also, no multi-organ approach has been tested before, in order to understand which systems are the most likely targets for AgNPs deposition and effects.

As such, we aimed to perceive if the injection of Sprague-Dawley rats with a low dose of AgNPs would cause long-term harmful effects in the animals' hepatic, cardiac and renal mitochondrial populations. We have concluded that, due to its functions as a detoxificating organ, the liver mitochondria are the prime targets for AgNPs effects and, even when exposed to a very low dose, a larger period of time is sufficient to cause lasting, measurable alterations. The supplementation of the AgNPs injections with a known antioxidant *N*-acetyl-*L*-cysteine (NAC) was effective in preventing most of the evaluated alterations.

2. Materials and Methods:

2.1. Materials

Unless otherwise noted, all materials and reagents were purchased from Sigma-Aldrich (St. Louis, MO) and were of the highest grade of purity commercially available. AgNPs (spherical, sodium citrate-coated 10 and 75nm diameter) were purchased from Nanocomposix (San Diego, CA). Lot references for AgNPs were DAG1856 (10 nm) and JME1038 (75 nm).

2.2. Animal care and experimental procedure

30 10-week old Sprague Dawley male rats were purchased from Charles River Laboratories (Barcelona, Spain). Animals were divided into groups of 5 per cage, with free access to standard rodent chow and acidified water (0.1 % (v/v) of a 25 % (v/v) HCl solution). Animals were kept in a temperature (25 ºC) and humidity controlled room, with a 12 h light/dark cycle. Animals were allowed to acclimate to the room for one week before the experimental procedure began.

Each cage animals were treated similarly, giving rise to 5 experimental groups, which were intraperitoneally (i.p.) injected with: a) Control, equivalent volume of phosphate buffer saline (PBS); b) 10 nm, 250 µg/Kg (w/w) of AgNPs 10 nm diameter; c) 75 nm, 250 µg/Kg (w/w) of AgNPs 75 nm diameter; d) 10 NAC, similar to group b), but 30 min before AgNPs injection

animals were i.p. injected with 100 mg/Kg (w/w) NAC; e) 75 NAC, similar to group c), but 30 min before AgNPs injection animals were i.p. injected with 100 mg/Kg (w/w) NAC.

The animals were treated once a week, for four weeks (i.e., 4 single doses of 250 µg/Kg of AgNPs for a final dosage of 1 mg/Kg in one month). During this period various parameters were controlled, and plasma was collected by tail bleeding at the beginning and end of the experimental protocol. After completing exactly 4 weeks from the first injection, animals were sacrificed by cervical dislocation and decapitation, with arterial blood being collected for analysis. Animals' liver, heart and kidneys were quickly removed, with samples collected for various purposes, being stored in specific buffers or in liquid N_2, as required.

2.3. Mitochondrial isolation

Mitochondria were isolated by using a previously described protocol ([20]), with modifications ([21]), always conducted at 4 ºC or in pelleted ice. Briefly, the kidneys were decapsulated and minced thinly. Heart and liver were also thinly minced with scissors and scalpels, in ice-cold Homogenization Buffer (250 mM Sucrose, 10 mM HEPES pH 7.4, 0.5 mM EGTA and 0.1% fat-free bovine serum albumin, BSA). Buffer was refreshed 3-4 times to remove excess blood from tissue. Tissues were homogenized with a Teflon piston and a Potter-Elvehjem homogenizer, at 300 rpm, in approximately 10 volumes of Homogenization Buffer. Homogenates were then spun at 2500 x*g* for 10 min. The resulting supernatant was placed into new tubes and centrifuged at 10 000 x*g* for 10 min, which results in a mitochondrial pellet. This pellet was resuspended in Washing Buffer (250 mM Sucrose, 10 mM HEPES pH 7.4) and centrifuged at 10 000 x*g* for 10 min. This last step was repeated twice, resulting in an ultra-pure mitochondrial fraction. Mitochondria were gently resuspended in a small volume of Washing buffer, and its protein content was quantified by the biuret method ([22]), calibrated with BSA.

2.4. Mitochondrial oxygen consumption

Oxygen consumption of isolated mitochondria was polarographically determined with a Clark-type oxygen electrode ([23]). Mitochondria (1 mg for liver, 0.5 mg for heart and kidney) were used. Reactions were carried out at 25 ºC, in a temperature-controlled water-jacketed chamber with magnetic stirring, in 1.4 mL of Respiratory Buffer (130 mM Sucrose, 50 mM KCl, 5 mM $MgCl_2$, 5 mM KH_2PO_4, 50 µM EDTA and 5 mM HEPES pH 7.4), supplemented with 2 µM Rotenone. Mitochondria were energized with 5 mM Succinate and State 3 respiration was induced by adding 200 nmol ADP. O_2 consumption was further evaluated in the presence of 0.5 µg Oligomycin and 1 µM carbonylcyanide-*p*-trifluoromethoxyphenylhydrazon (FCCP).

2.5. Mitochondrial membrane potential ($\Delta\psi$) evaluation

$\Delta\psi$ was estimated using an ion-selective electrode to measure the distribution of tetraphenylphosphonium (TPP^+) according to previously established methods ([24]; [21]). The voltage response of the TPP^+ electrode to log [TPP^+] was linear with a slope of 59 ± 1, in conformity with the Nernst equation. Reactions were carried out at 25 ºC, in a temperature-controlled water-jacketed chamber with magnetic stirring, in 1.4 mL of Respiratory Buffer, supplemented with 3 µM TPP^+, 2 µM Rotenone and 5 mM Succinate. Reactions were initiated by the addition of mitochondria. A matrix volume of 1.1 µL/mg protein was assumed.

2.6. Plasma assays

Blood plasma was collected as mentioned before into ice-cold 0.5 M EGTA tubes and centrifuged at 4 ºC for 5 min at 10 000 x*g*. Resulting supernatant was used for the following assays.

Aspartate Aminotransferase (AST), Lactate Dehydrogenase and Alanine Aminotransferase (ALT) detection kits were purchased from Hospitex Diagnostics (Florence, Italy), and performed following manufacturer's instructions.

2.7. Reactive oxygen species generation

ROS generation was fluorometrically determined using a Victor^3 plate-reader (PerkinElmer, Waltham, MA), recording excitation and emission wavelengths of 485 and 538 nm, respectively, which correspond to the functional wavelengths of 2'.7'-Dichlorodihydrofluorescein diacetate (H_2DCFDA) ([25]). Isolated mitochondria (1 mg for liver, 0.5 mg for heart and kidney) were suspended in Respiratory buffer and loaded with 5 mM Succinate and 50 µM H_2DCFDA (prepared in DMSO) for 15 min, in the dark at 25 ºC. Mitochondria were then centrifuged at 3000 x*g* for 3 min and resuspended in 1 mL of fresh Respiratory buffer, in order to eliminate excess probe that did not enter mitochondria. 200 µL of this mitochondrial preparation were then loaded into a 96-well plate and the fluorescence was recorded for 20 min, both at a basal level and in the presence of 0.1 µg Antimycin A, for maximal ROS generation rate. The results are expressed as arbitrary relative fluorescence units (RFU's).

2.8. ATP quantification

Adenosine nucleotide extraction was performed as before ([26]). Briefly, tissue samples (20 mg) were pulverized with a ceramic mortar and pestle in liquid N_2 and homogenized in 25 µL of ice-cold KOH buffer (KOH 2.5 M, K_2HPO_4 1.5 M). Homogenates were vortexed and centrifuged at 14 000 x*g* for 2 min, at 4 ºC. The supernatants were collected and dissolved in 200 µL of K_2HPO_4 1M, with the pH adjusted to 7 with HCl. Samples were stored at -80 ºC for posterior quantification, following the instructions of the manufacturer of an ATP bioluminescent assay kit (Sigma-Aldrich) on a Victor^3 plate reader.

2.9. Enzymatic activities

Succinate Dehydrogenase (SDH) activity was polarographically determined as previously described ([27]). The reaction was carried out at 25 ºC in 1.4 mL of Respiratory Buffer supplemented with 5 mM Succinate, 2 µM Rotenone, 0.1 µg Antimycin A, 1 mM KCN and 0.3 mg Triton X-100. After the addition of freeze-thawed mitochondria (0.25 mg), the reaction was initiated by adding 1 mM Phenazine Methosulfate (PMS).

Cytochrome *c* Oxidase (COX) activity was polarographically determined as previously described ([28]). The reaction was carried out at 25 ºC in 1.4 mL of Respiratory Buffer supplemented with 2 µM Rotenone, 10 µM oxidized Cytochrome *c* and 0.3 mg Triton X-100. After the addition of freeze-thawed mitochondria (0.25 mg), the reaction was initiated by adding 5 mM Ascorbate plus 0.25 mM Tetramethulphenylene-diamine (TMPD).

ATPase activity of ATPSynthase was spectrophotometrically determined at 660 nm, by recording ATP hydrolysis as previously described ([29]). The reaction was carried in test tubes at 37 ºC containing 2 mM of ATPase reaction buffer (125 mM Sucrose, 65 mM KCl, 2.5 mM $MgCl_2$ and 0.5 mM HEPES, pH 7.4). After the addition of freeze-thawed mitochondria (0.25 mg), the reaction was initiated by the addition of 2 mM Mg^{2+}-ATP, in either the presence or absence of 0.25 µg Oligomycin. After 10 min, the reaction was stopped by the addition of 1 mL of 40 % Trichloroacetic acid and placed on ice. Samples were then vortexed and 1 mL of the reaction volume was added to new tubes containing 2 mL Molibdate reagent 10% in H_2SO_4 10N and 2 mL H_2O. Tubes were allowed to react for 3 min and absorbance was measured. ATPase activity was calculated as the difference in total absorbance and absorbance in the presence of the specific ATPSynthase inhibitor Oligomycin.

2.10. Measurement of the mitochondria permeability transition

Mitochondrial swelling was estimated by changes in light scattering, as spectrophotometrically monitored at 540 nm ([30]). Reactions were carried at 25 ºC. Recording was initiated by the addition of mitochondria (1 mg for liver, 0.5 mg for heart and kidney) to 2 mL of Swelling buffer (200 mM Sucrose, 10 mM Tris-MOPS, 1 mM KH_2PO_4, 10 µM EGTA pH 7.4), supplemented with 3 µM Rotenone and 5 mM Succinate. After a brief period of basal absorbance recording, different amounts of $CaCl_2$ were added, and the resulting alterations in light scattering were recorded.

2.11. Measurement of mitochondrial calcium fluxes

The accumulation and release of calcium by isolated mitochondria was determined using a calcium-sensitive fluorescent dye, Calcium Green-5 N

(Life Technologies, San Diego, CA), as previously described ([31]). The reactions were carried out at 25 ºC in 2 mL of Respiratory buffer, supplemented with 3 µM Rotenone and 0.5 µg Oligomycin. Free Ca^{2+} was monitored by using 100 nM Calcium Green added to the reaction with 0.5 mg of mitochondria.

2.12. Western blotting analysis

Western blot analysis of specific protein content was performed as before ([26]). Briefly, flash-frozen tissue samples were lysed in ice-cold RIPA lysis buffer (50 mM Tris, 150 mM NaCl, 0.1 % SDS, 0.5% sodium deoxycholate, 1% Triton X-100) supplemented with a cocktail of protease and phosphatase inhibitors. Equal amounts of protein (quantified with a Bicinchoninic acid kit) were loaded and electrophoresed on a home-made SDS-polyacrylamide gel and transferred to a polyvinylidene difluoride membrane (Bio-Rad Laboratories, Hercules, CA). Membranes were blocked with 5% Blocking solution (Bio-Rad) for 2h and incubated with a primary antibody in Tris-buffered saline (TBS) supplemented with 1% Tween-20 (TBS-T) and 0.5% blocking solution overnight at 4 ºC with constant rolling stir. Primary antibodies used were as follows: ß-Actin (Sigma-Aldrich); COX-I (Mitosciences, Eugene, OR); COX-IV (Mitosciences). The following day, membranes were washed in room temperature TBS-T 3 times for 30 min and incubated with a corresponding secondary antibody (Life Technologies). Membranes were then washed with room temperature TBS-T 3 times for 15 min. Immunodetection was performed with a WesternDot 625 goat anti-rabbit or anti-mouse western blot kits (Life Technologies). Membranes were then imaged using a Gel-Doc EZ instrument (Bio-Rad). Densitometric analysis was performed with ImageJ ([32]).

2.13. Statistical analysis

Data are represented as a mean of $n \geq 4 \pm$ SEM, and statistical significance was determined using the one-way (two-way for swelling and Calcium green tests) ANOVA test with a Bonferroni correction (GraphPad Prism, La Jolla, CA). A p value of < 0.05 was considered statistically significant.

3. Results

3.1. Animal characterization

As is visible in Fig. 1, the animals followed a similar pattern of both weight gain (Fig. 1A) and food intake (Fig. 1B). In the week of the start of the treatments, the 10 nm group had already gained a significant different weight and food intake when compared with the other groups. However, since this pattern was stable throughout the study and emerged after animal sorting but before treatment initiation, we conclude that the treatments did not affect animals' body weight nor food intake, and these differences are accountable to natural animal variability ([33]).

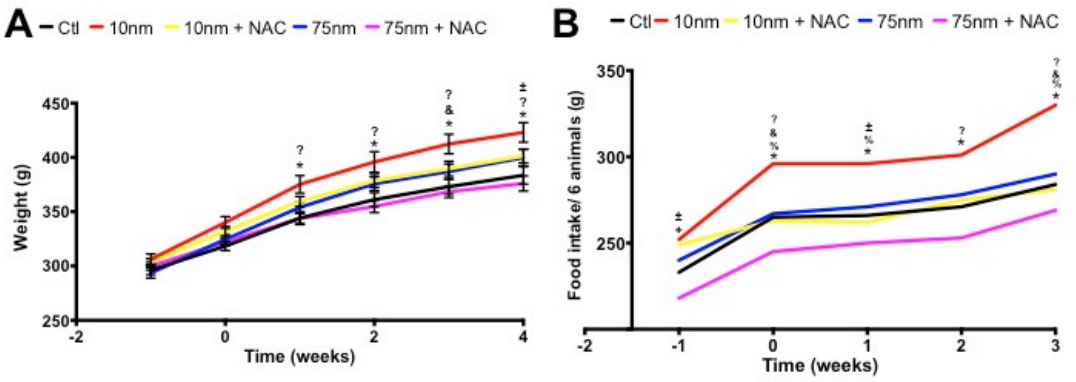

Fig. 1 – Total body weight (A) and food intake (B) progression during the study.

3.2. Blood plasma characterization

In order to better understand possible toxic effects of AgNPs that would be detectable on a routine blood work, we conducted an evaluation of the plasmatic levels of common indicators of organ damage, the presence of AST, ALT and LDH. As seen in Fig. 2, no alterations were found in ALT levels due to the treatments (Fig. 2A). However, NAC supplementation allowed for a significant decrease in AST levels in animals exposed to 10 nm AgNPs (Fig.

2B). In terms of LDH release, both 10 and 75 nm AgNPs caused a significant increase in the presence of this enzyme in plasma (Fig. 2C), an effect rescued by NAC supplementation.

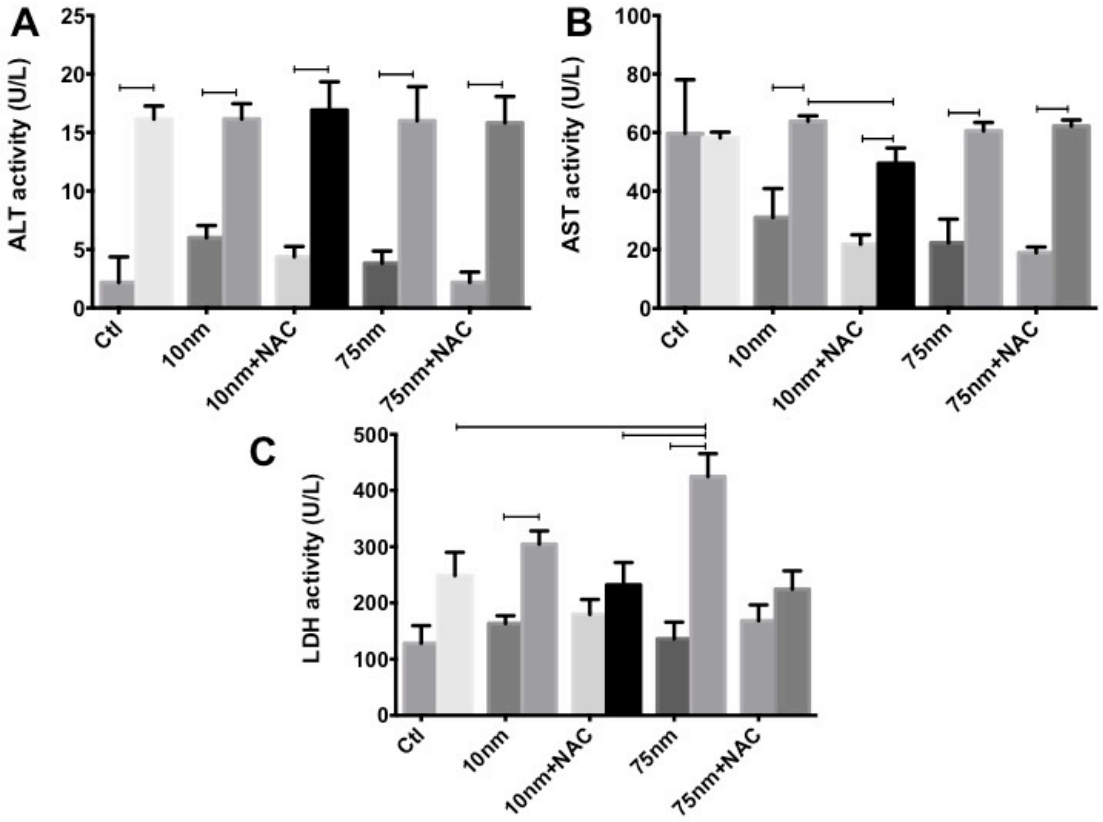

Fig. 2 – Plasmatic levels of ALT (A), AST (B) and LDH (C).

3.3. Liver mitochondria

3.3.1. Mitochondrial membrane potential ($\Delta\psi$)

In order to understand if AgNPs exposure caused any long-term effects of hepatic mitochondrial function, we assessed several functional parameters with the resource to a TPP^+ electrode. As seen in Fig. 3A and C, both 10 and 75 nm AgNPs caused a NAC-reversible decrease in mitochondrial initial and repolarization potentials, respectively. This is accompanied by a significant, similarly NAC-reversible, increase in the lag phase time (Fig. 3D). Also, in terms of depolarization potential (Fig. 3B), both AgNPs sizes caused a

significant reduction, which was not recovered by NAC. These data clearly indicate that AgNPs, at this low-dose, are sufficient to compromise hepatic mitochondrial function.

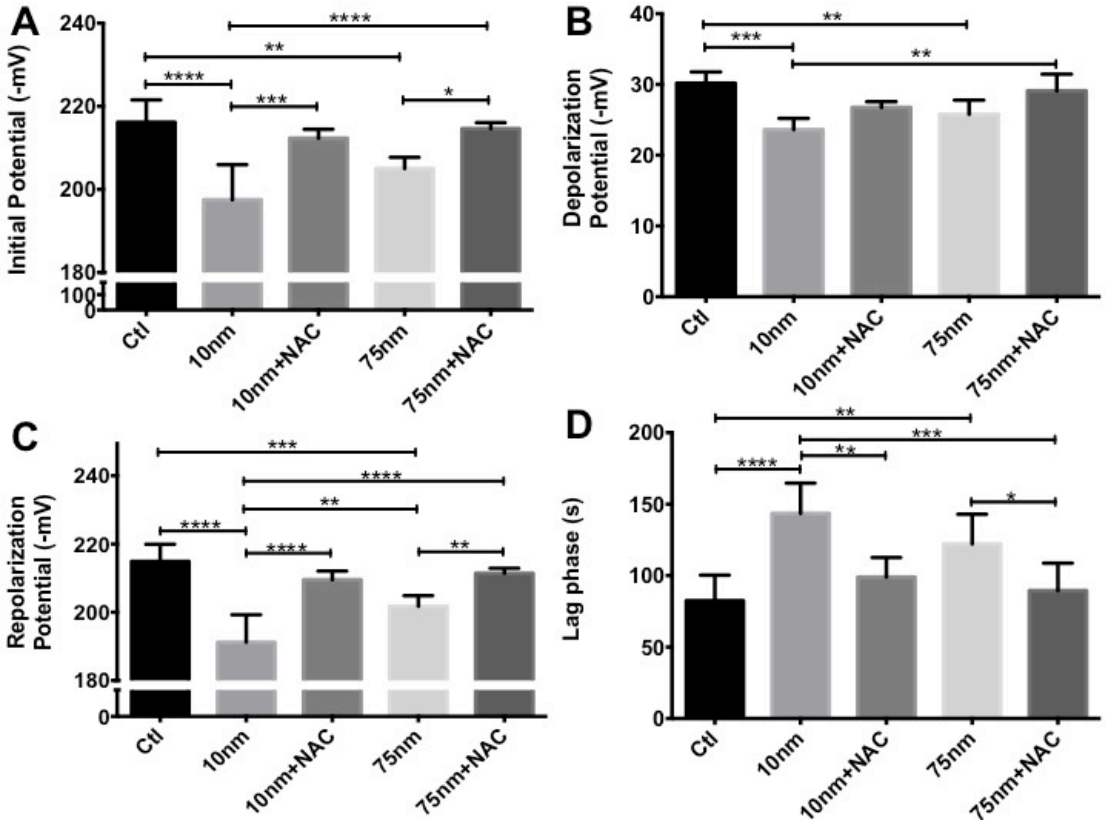

Fig 3 – Hepatic mitochondrial membrane potentials (∆ψ) and lag phase. Initial potential (A), Depolarization potential (B), Repolarization potential (C) and Lag phase time (D).

3.3.2 Mitochondrial respiration

Since mitochondria utilize oxygen to generate the membrane potential required for ATP generation, we evaluated the O_2 disappearance rate in the isolated mitochondria. As it is visible in Fig. 4A, AgNPs treatment (for both sizes) caused a NAC-reversible decrease in ADP-stimulated State 3 respiration, which is in accordance with the data from membrane potential (Fig. 3). Curiously, only 75 nm AgNPs caused a significant increase in State 4 respiration, indicating that these AgNPs created a pronounced protonic leak issue across the inner mitochondrial membrane (Fig. 4B). This is further

confirmed by the fact that respiration in the presence of the ATPSynthase inhibitor Oligomycin is also elevated by AgNPs treatment (Fig. 4C). However, this effect was only salvaged by NAC in the 75 nm AgNPs, hinting to the fact that 10 nm AgNPs cause irreversible damage to hepatic mitochondrial ATPSynthase complexes. Regardless, taking into account all these previous data, it is clear that the phosphorylative system of hepatic mitochondria is damaged by both sizes of AgNPs, since both 10 and 75 nm AgNPs caused a significant reduction on FCCP-stimulated mitochondrial respiration (Fig. 4D), an effect not totally salvaged by NAC supplementation.

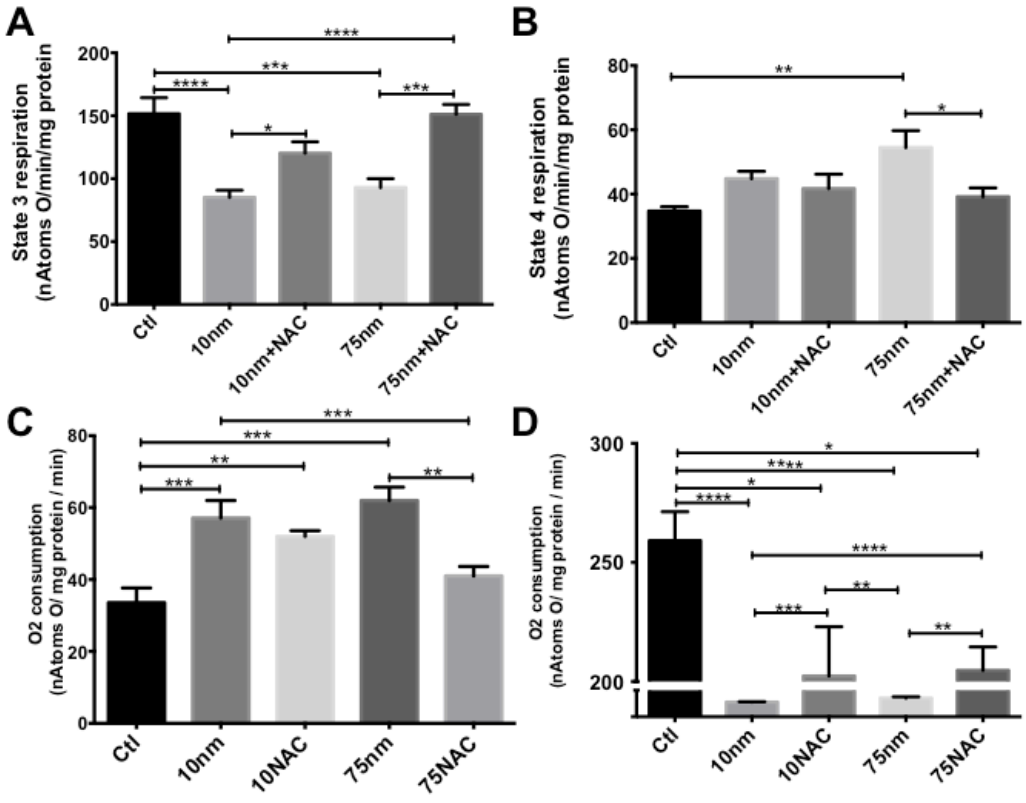

Fig. 4 – Hepatic mitochondrial respiration. State 3 respiration (A), State 4 respiration (B), Respiration in the presence of ADP and oligomycin (C) and FCCP-induced respiration (D).

The data from mitochondrial respiration can be further explored into the creation of the highly informative Respiratory Control (RCR) and ADP/O ratios. RCR is calculated by dividing State 3 by State 4, indicating a ratio of ADP-

driven function by normalizing it against the mitochondrial resting respiration, while the ADP/O ratio indicates the number of ADP molecules by one atom of oxygen consumed, indicating the efficiency of mitochondria. Fig. 5 demonstrates these ratios.

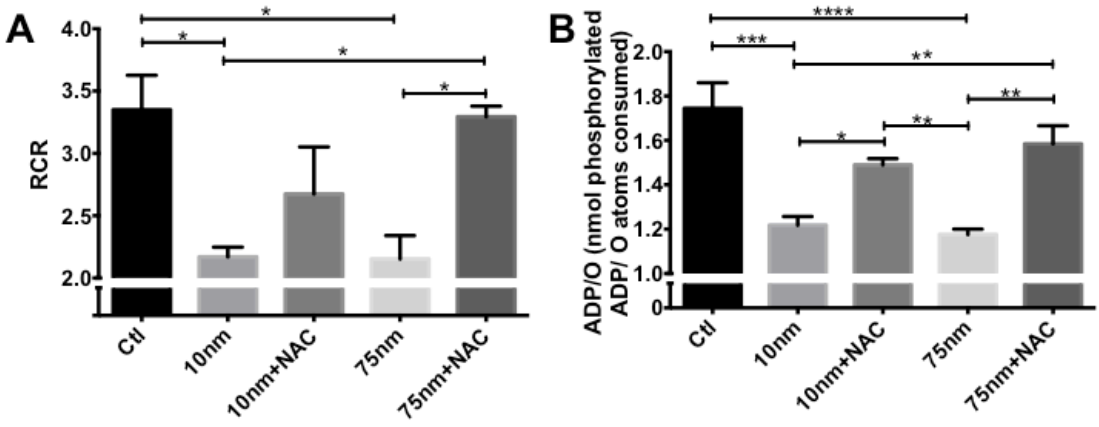

Fig. 5 – Hepatic mitochondrial respiration RCR (A) and ADP/O (B) ratios.

As it would be expected, the reduction in State 3 respiration caused by AgNPs results in a decrease in the RCR, which coupled with the increase in State 4 respiration for 75 nm, ends in NAC salvaging RCR for 75 nm AgNPs (Fig. 5A). In accordance with the previous data, ADP/O is unsurprisingly diminished in AgNPs mitochondria, being salvaged by NAC (Fig. 5B). As such, all *ex vivo* mitochondrial analyses point to the fact that both 10 and 75 nm AgNPs cause a NAC-preventable hepatic mitochondrial dysfunction.

3.3.3 Mitochondrial calcium fluxes and swelling

Mitochondrial swelling was evaluated by presenting 10 nmol Ca^{2+} to mitochondrial preparations. Resulting data is presented in Fig. 6. As can be seen, for all assays, the pretreatment of mitochondria with the inhibitor of the mitochondrial permeability transition (mPT) pore (mPTP) Cyclosporine A (CyA) totally prevents mPTP induction and thus mitochondrial swelling. For both 10 (Fig. 6A) and 75 nm AgNPs (Fig. 6B), 10 nmol of Ca^{2+} was sufficient to induce rapid mitochondrial swelling, which NAC prevented. In fact NAC-

pretreated AgNPs' injected mitochondria behave exactly as do the control animals' mitochondria. The same protective effect was also visible when mitochondria were exposed to 20 nmol Ca^{2+}, albeit the protective effect of NAC was less intense (data not shown).

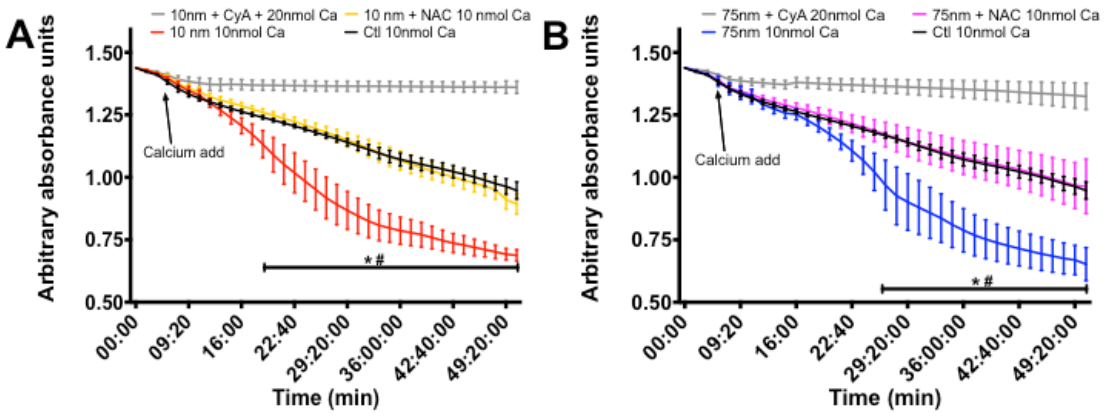

Fig. 6 – Hepatic mitochondrial swelling of 10 (A) and 75 nm AgNPs (B).

Interestingly, when the Ca^{2+}-sensitive fluorescent probe Calcium Green-5N was used to study calcium fluxes, we uncovered no difference whatsoever, independently of amount calcium used and mitochondria preparation (data not shown).

3.3.4 Mitochondrial ROS generation evaluation

In order to better understand if AgNPs are causing mitochondrial dysfunction by increasing reactive oxygen species (ROS) generation and if the antioxidant effects of NAC are responsible for its salvaging effect, we investigated ROS generation on isolated hepatic mitochondria. The results are summarized in Fig. 7. Unsurprisingly, both 10 and 75 nm AgNPs caused an elevation of ROS generation when compared with control mitochondria, both when measuring mitochondria in a basal state (Fig. 7A) and when mitochondria are forced to increase ROS generation by the addition of the Complex III inhibitor, Antimycin A (Fig. 7B). Remarkably, despite a clear trend

towards a decrease in ROS generation caused by NAC pretreatment, no statistically significant differences were found, a fact we attribute to the rather elevated data scatter.

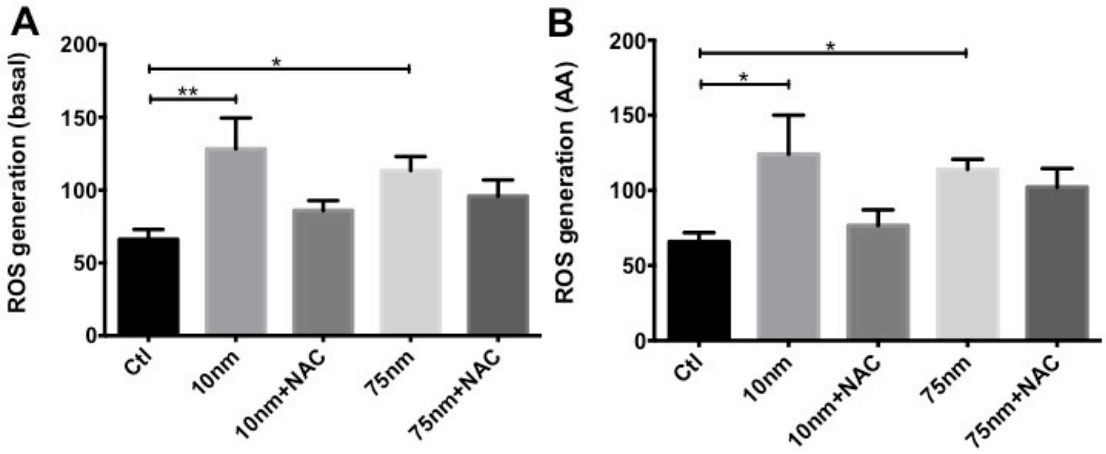

Fig. 7 – Hepatic mitochondrial ROS generation in the basal state (A) and in the presence of Antimycin A (B).

3.3.5 Mitochondrial respiratory complexes activities

As consequence of the several alterations found in mitochondrial assays, we assessed the specific activities of mitochondrial respiratory chain complexes. As is visible in Fig. 8, Complex II (Succinate Dehydrogenase, SDH) activity was significantly affected by both sizes of AgNPs (Fig. 8A). However, despite a clear trend towards a beneficial effect of NAC on 10 nm AgNPs, NAC was only statistically efficient in recovering SDH activity from 75 nm AgNPs. In contrast, Complex IV (Cytochrome *c* Oxidase, COX) activity was significantly affected by both sizes of AgNPs and NAC rescued these effects, independently of AgNPs size (Fig. 8B). In contrast with COX and similarly to SDH, the ATPase activity of the mitochondrial ATP Synthase was irreversibly reduced by 10 nm AgNPs, and not by 75 nm AgNPs (Fig. 8C).

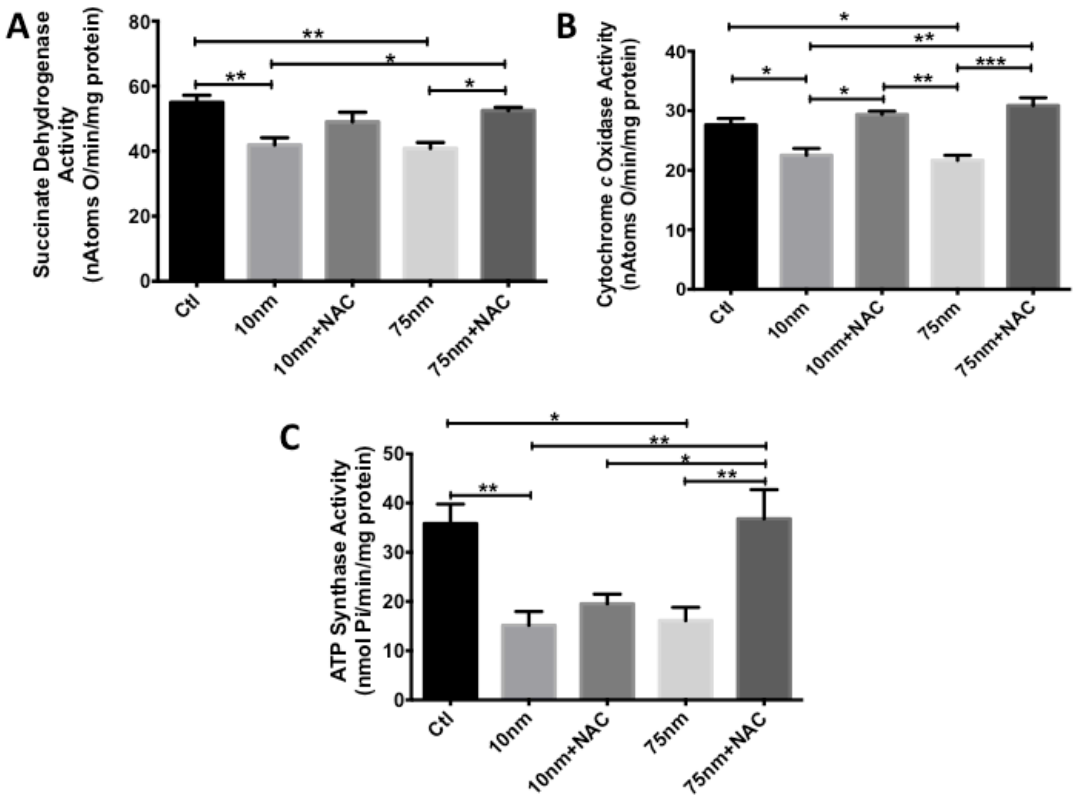

Fig. 8 – Hepatic mitochondrial complex activities of Succinate Dehydrogenase (A), Cytochrome *c* Oxidase (B) and ATP Synthase (C).

3.3.6 Hepatic ATP content

Due to the perceived alterations in mitochondrial activity, we evaluated ATP content in liver samples. Contrarily to what would be expected, we found no statistical alterations in ATP content from all groups of treatments (data not shown), which indicates that these alterations are not (at least not yet) affecting hepatic energetic necessities.

3.3.7 Hepatic protein content

Due to the data above described, we tried to understand if the presence of AgNPs were affecting mitochondrial numbers in hepatic cells. To do just that, we evaluated the liver content of mitochondrial proteic complex, COX. By evaluating the presence of both a mitochondrially DNA-encoded

(COX-I) and a nuclearly DNA-encoded (COX-IV) subunit, we can assess if there are alterations to the expression of any DNA in terms of mitochondrial protein production. As is visible in Fig. 9, there is a non-statistical trend towards increased COX-I and COX-IV content in the livers of animals exposed to both 10 and 75 nm AgNPs. This was countered by NAC at COX-IV level, for the 75 nm AgNPs (Fig. 9B). We propose that this trend is caused by the deficient mitochondrial capacity of AgNPs-exposed mitochondria to generate ATP, which leads the cells to try to compensate by producing more functional units to try to counter the lack of efficiency. As such, we believe that, in light of all the above data, we are witnessing an attempt by the liver to cope with the mitochondrial insults caused by AgNPs. This would explain why there are so many alterations in efficiency but no differences in ATP levels are found.

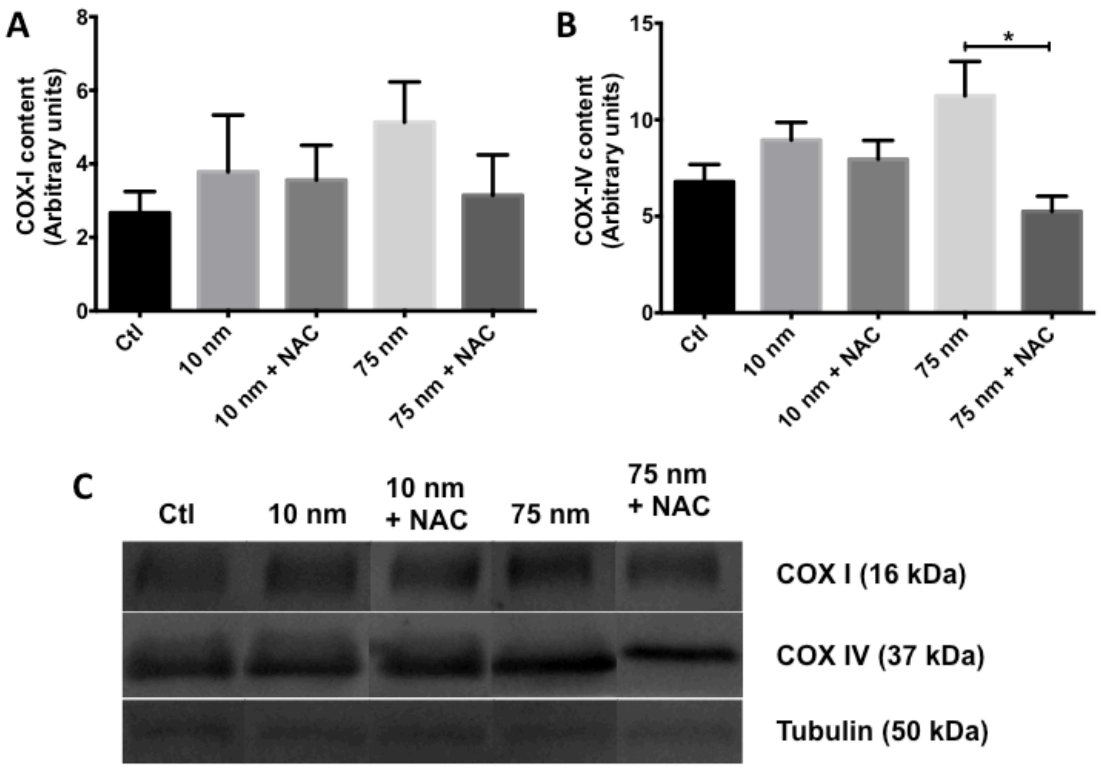

Fig. 9 – Hepatic levels of Cytochrome *c* oxidase subunits, COX-I (A) and COX-IV (B), with representative Western Blot figures (C).

3.4 Heart mitochondria

All of the above assays were also conducted in heart mitochondria. We found no alterations in any of the above parameters (data not shown) except for mitochondrial swelling.

As can be seen in Fig. 10, 10 nm AgNPs caused a significant deleterious effect on cardiac mitochondria capacity to accumulate calcium ions, an effect reversed by NAC (Fig. 10A). However, virtually no differences were found when discussing 75 nm AgNPs.

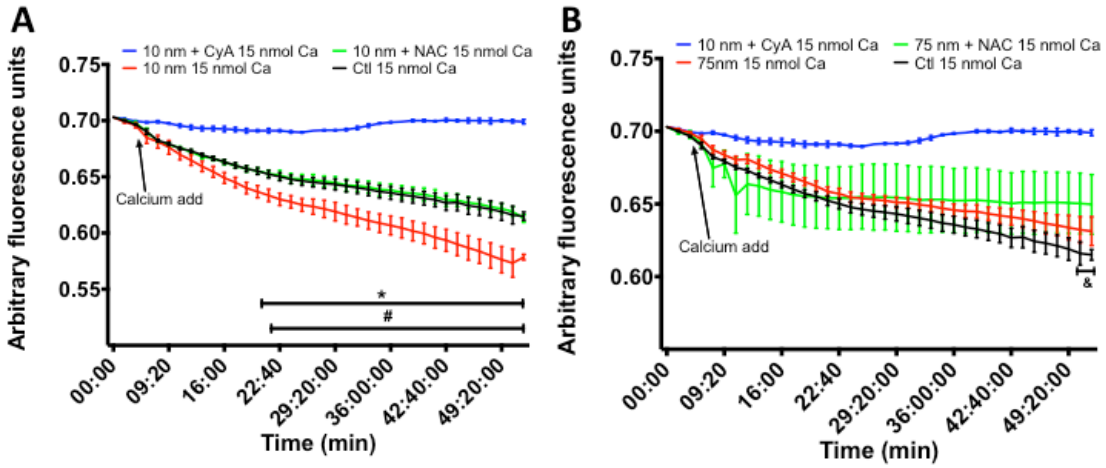

Fig. 10 – Cardiac mitochondrial swelling of 10 (A) and 75 nm AgNPs (B).

The lack of alterations indicates that cardiac mitochondria are more resilient to AgNPs-induced damaged than hepatic mitochondria, at least for the tested dosages and time frame.

3.5 Renal mitochondria

Just like with cardiac mitochondria, all of the above assays were conducted with renal mitochondria. And, just like in the heart, mitochondria isolated from the kidneys of AgNPs-injected animals demonstrated absolutely no differences when all groups were compared. This comes as no surprise,

since renal mitochondria are one the most resilient and damage-resistant mitochondria in the organism (data not shown).

4. Conclusion

Given the above data, we can conclude that even a low-dose, chronic exposure to AgNPs can cause severe impediments to normal mitochondrial function, at least at a hepatic level. Despite no alterations were found in heart and kidney levels, and despite the fact that the alterations found in liver mitochondria did not appear to compromise ATP generation, it is not possible (and, in fact, it is probably unadvisable) to rule out any harmful effects of AgNPs, even in a low dose, to the organism.

5. References

[1] N. Singh, B. Manshian, G. J. S. Jenkins, S. M. Griffiths, P. M. Williams, T. G. G. Maffeis, C. J. Wright, and S. H. Doak, “NanoGenotoxicology: the DNA damaging potential of engineered nanomaterials.,” *Biomaterials*, vol. 30, no. 23, pp. 3891–3914, Aug. 2009.

[2] C. Carlson, S. M. Hussain, A. M. Schrand, L. K. Braydich-Stolle, K. L. Hess, R. L. Jones, and J. J. Schlager, “Unique cellular interaction of silver nanoparticles: size-dependent generation of reactive oxygen species.,” *J Phys Chem B*, vol. 112, no. 43, pp. 13608–13619, Oct. 2008.

[3] T. Bartłomiejczyk and A. Lankoff, “Silver nanoparticles–allies or adversaries,” *Annals of Agricultural …*, 2013.

[4] J. S. Teodoro, A. M. Simões, F. V. Duarte, A. P. Rolo, R. C. Murdoch, S. M. Hussain, and C. M. Palmeira, “Assessment of the toxicity of silver nanoparticles in vitro: a mitochondrial perspective.,” *Toxicol In Vitro*, vol. 25, no. 3, pp. 664–670, Apr. 2011.

[5] M. Ahamed, M. S. Alsalhi, and M. K. J. Siddiqui, “Silver nanoparticle applications and human health.,” *Clin. Chim. Acta*, vol. 411, no. 23, pp. 1841–1848, Dec. 2010.

[6] C. S. Costa, J. V. V. Ronconi, J. F. Daufenbach, C. L. Gonçalves, G. T. Rezin, E. L. Streck, and M. M. D. S. Paula, “In vitro effects of silver nanoparticles on the mitochondrial respiratory chain.,” *Mol Cell Biochem*, vol. 342, no. 1, pp. 51–56, Sep. 2010.

[7] T. M. Tolaymat, A. M. El Badawy, A. Genaidy, K. G. Scheckel, T. P. Luxton, and M. Suidan, “An evidence-based environmental perspective of manufactured silver nanoparticle in syntheses and applications: a systematic review and critical appraisal of peer-

reviewed scientific papers.," *Sci. Total Environ.*, vol. 408, no. 5, pp. 999–1006, Feb. 2010.

[8] R. Zhang, M. J. Piao, K. C. Kim, A. D. Kim, J.-Y. Choi, J. Choi, and J. W. Hyun, "Endoplasmic reticulum stress signaling is involved in silver nanoparticles-induced apoptosis.," *Int. J. Biochem. Cell Biol.*, vol. 44, no. 1, pp. 224–232, Jan. 2012.

[9] A. Sarkar, M. Ghosh, and P. C. Sil, "Nanotoxicity: oxidative stress mediated toxicity of metal and metal oxide nanoparticles.," *J Nanosci Nanotechnol*, vol. 14, no. 1, pp. 730–743, Jan. 2014.

[10] J. Sengupta, S. Ghosh, P. Datta, A. Gomes, and A. Gomes, "Physiologically important metal nanoparticles and their toxicity.," *J Nanosci Nanotechnol*, vol. 14, no. 1, pp. 990–1006, Jan. 2014.

[11] M. Zhang, J. Jin, Y. N. Chang, and X. Chang, "Toxicological Properties of Nanomaterials," *Journal of Nanoscience …*, 2014.

[12] Y. Baratli, A.-L. Charles, V. Wolff, L. Ben Tahar, L. Smiri, J. Bouitbir, J. Zoll, F. Piquard, O. Tebourbi, M. Sakly, H. Abdelmelek, and B. Geny, "Impact of iron oxide nanoparticles on brain, heart, lung, liver and kidneys mitochondrial respiratory chain complexes activities and coupling.," *Toxicol In Vitro*, vol. 27, no. 8, pp. 2142–2148, Dec. 2013.

[13] M. Korani, S. M. Rezayat, and S. Arbabi Bidgoli, "Sub-chronic Dermal Toxicity of Silver Nanoparticles in Guinea Pig: Special Emphasis to Heart, Bone and Kidney Toxicities.," *Iran J Pharm Res*, vol. 12, no. 3, pp. 511–519, 2013.

[14] J. S. Teodoro, A. P. Rolo, and C. M. Palmeira, "The NAD ratio redox paradox: why does too much reductive power cause oxidative stress?," *Toxicology Mechanisms and Methods*, vol. 23, no. 5, pp. 297–302, Jun. 2013.

[15] D. C. Wallace, "Bioenergetic origins of complexity and disease.," *Cold Spring Harb. Symp. Quant. Biol.*, vol. 76, pp. 1–16, 2011.

[16] J. N. Meyer, M. C. K. Leung, J. P. Rooney, A. Sendoel, M. O. Hengartner, G. E. Kisby, and A. S. Bess, "Mitochondria as a target of environmental toxicants.," *Toxicological Sciences*, vol. 134, no. 1, pp. 1–17, Jul. 2013.

[17] O. F. Karataş, E. Sezgin, O. Aydin, and M. Culha, "Interaction of gold nanoparticles with mitochondria.," *Colloids Surf B Biointerfaces*, vol. 71, no. 2, pp. 315–318, Jul. 2009.

[18] M. A. Siddiqui, H. A. Alhadlaq, J. Ahmad, A. A. Al-Khedhairy, J. Musarrat, and M. Ahamed, "Copper oxide nanoparticles induced mitochondria mediated apoptosis in human hepatocarcinoma cells.," *PLoS ONE*, vol. 8, no. 8, p. e69534, 2013.

[19] E. Bressan, L. Ferroni, C. Gardin, C. Rigo, M. Stocchero, V. Vindigni, W. Cairns, and B. Zavan, "Silver nanoparticles and mitochondrial interaction.," *Int J Dent*, vol. 2013, p. 312747, 2013.

[20] P. Gazotti, K. Malmstron, and M. Crompton, "[CITATION][C]," *… biochemistry Springer-Verlag New York Inc*, 1979.

[21] C. M. Palmeira, A. J. Moreno, and V. Madeira, "Interactions of herbicides 2, 4-D and dinoseb with liver mitochondrial bioenergetics," *Toxicology and applied …*, 1994.

[22] A. G. GORNALL, C. J. BARDAWILL, and M. M. DAVID, "Determination of serum proteins by means of the biuret reaction.," *J*

Biol Chem, vol. 177, no. 2, pp. 751–766, Feb. 1949.
[23] R. W. Estabrook, "[CITATION][C]," *Meth. Enzymol.*, 1967.
[24] N. Kamo, M. Muratsugu, R. Hongoh, and Y. Kobatake, "Membrane potential of mitochondria measured with an electrode sensitive to tetraphenyl phosphonium and relationship between proton electrochemical potential and phosphorylation potential in steady state.," *J. Membr. Biol.*, vol. 49, no. 2, pp. 105–121, Aug. 1979.
[25] S. Zhou, C. Palmeira, and K. Wallace, "Doxorubicin-induced persistent oxidative stress to cardiac myocytes," *Toxicol Lett*, vol. 121, no. 3, pp. 151–157, 2001.
[26] J. S. Teodoro, F. V. Duarte, A. P. Gomes, A. T. Varela, F. M. Peixoto, A. P. Rolo, and C. M. Palmeira, "Berberine reverts hepatic mitochondrial dysfunction in high-fat fed rats: a possible role for SirT3 activation.," *Mitochondrion*, vol. 13, no. 6, pp. 1–10, Sep. 2013.
[27] T. P. Singer, "Determination of the activity of succinate, NADH, choline, and alpha-glycerophosphate dehydrogenases.," *Methods Biochem Anal*, vol. 22, pp. 123–175, 1974.
[28] D. L. Brautigan, S. Ferguson-Miller, and E. Margoliash, "Mitochondrial cytochrome c: preparation and activity of native and chemically modified cytochromes c.," *Meth. Enzymol.*, vol. 53, pp. 128–164, 1978.
[29] J. S. Teodoro, A. P. Rolo, F. V. Duarte, A. M. Simões, and C. M. Palmeira, "Differential alterations in mitochondrial function induced by a choline-deficient diet: understanding fatty liver disease progression.," *Mitochondrion*, vol. 8, no. 5, pp. 367–376, Dec. 2008.
[30] C. M. Palmeira and K. B. Wallace, "Benzoquinone inhibits the voltage-dependent induction of the mitochondrial permeability transition caused by redox-cycling naphthoquinones.," *Toxicology and Applied Pharmacology*, vol. 143, no. 2, pp. 338–347, Apr. 1997.
[31] P. J. Oliveira, A. P. Rolo, R. Seiça, C. M. Palmeira, M. S. Santos, and A. J. Moreno, "Decreased susceptibility of heart mitochondria from diabetic GK rats to mitochondrial permeability transition induced by calcium phosphate.," *Biosci. Rep.*, vol. 21, no. 1, pp. 45–53, Feb. 2001.
[32] M. D. Abràmoff and P. J. Magalhães, "Image processing with ImageJ," *Biophotonics …*, 2004.
[33] C. L. Gavaghan, J. K. Nicholson, S. C. Connor, and I. D. Wilson, "Directly coupled high-performance liquid chromatography and nuclear magnetic resonance spectroscopic with chemometric studies on metabolic variation in Sprague …," *Analytical …*, 2001.